Temporary denitrification in the Antarctic stratosphere as observed by ILAS-II in the 2003 early winter: *Comparison with a microphysical box model* ***(00107)***

Takafumi Sugita,[1] Sachiko Hayashida,[2] and Hitoshi Irie[3]

1. National Institute for Environmental Studies, Tsukuba, Japan
2. Nara Woman's University, Nara, Japan
3. FRCGC/JAMSTEC, Yokohama, Japan

- **Extended abstract (EA):** To examine the characteristics of polar stratospheric clouds (PSCs) in the Antarctic, we have analyzed short-time (within 5 days) changes in nitric acid (HNO_3) and aerosol extinction coefficient (AEC) at 780 nm, focusing near 20 km altitude in June 2003 as observed by the Improved Limb Atmospheric Spectrometer (ILAS)-II. The Match technique based on the air parcel trajectory was applied to the ILAS-II data. The several Match pairs have revealed decreased HNO_3 values with increased AEC values within the short times, indicating temporary denitrification. It is also suggested that the observed PSCs could be nitric acid trihydrate (NAT) particles, considering that the temperatures were above existence temperatures for supercooled ternary solution (STS), but below those for NAT. Given appropriate size distributions for NAT particles, it is suggested that the median radius of particles was less than 3 micron.

- **(EA cont'd):** For these cases where temporary denitrification by NAT particles were found, a Lagrangian microphysical box model (including nucleation, growth, and sedimentation) was used to calculate the temporal changes in HNO_3 along the Match trajectories. The model utilizes a mechanism that nucleation of nitric acid dihydrate (NAD) on STS droplet surfaces takes place and then instantaneous conversion of NAD nuclei into NAT occurs. A parameterization for the free energy of NAD nucleus formation on the STS surfaces will be discussed from a view point of HNO_3 variations between measurement and model results.
- **ILAS-II observations**: Vertical profiles of O_3, HNO_3, AEC@780 nm, as well as several trace molecules, in the high latitude stratosphere were observed with the Improved Limb Atmospheric Spectrometer (ILAS)-II from April to October 2003. ILAS-II utilizes the solar occultation method and was aboard the sun-synchronous polar-orbiting satellite, ADEOS-II.

- **Meteorological condition in June 2003:** The onset of denitrification was seen in this period [*Daerden et al.*, 2007]. A typical temperature condition at 490 K level reveals that most of the measurements were within 195 K. The measurement latitudes of ILAS-II were between 65 and 67°S, where most of the measurements were located innerly from the boundary of the polar vortex. (Ertel's PV value of the center boundary is around -41×10^{-6} $m^2s^{-1}kg^{-1}$ K, and that of mean $\pm1\sigma$ s.d. for the ILAS-II measurement locations is $-49.7\pm4.8\times10^{-6}$ $m^2s^{-1}kg^{-1}$ K.)

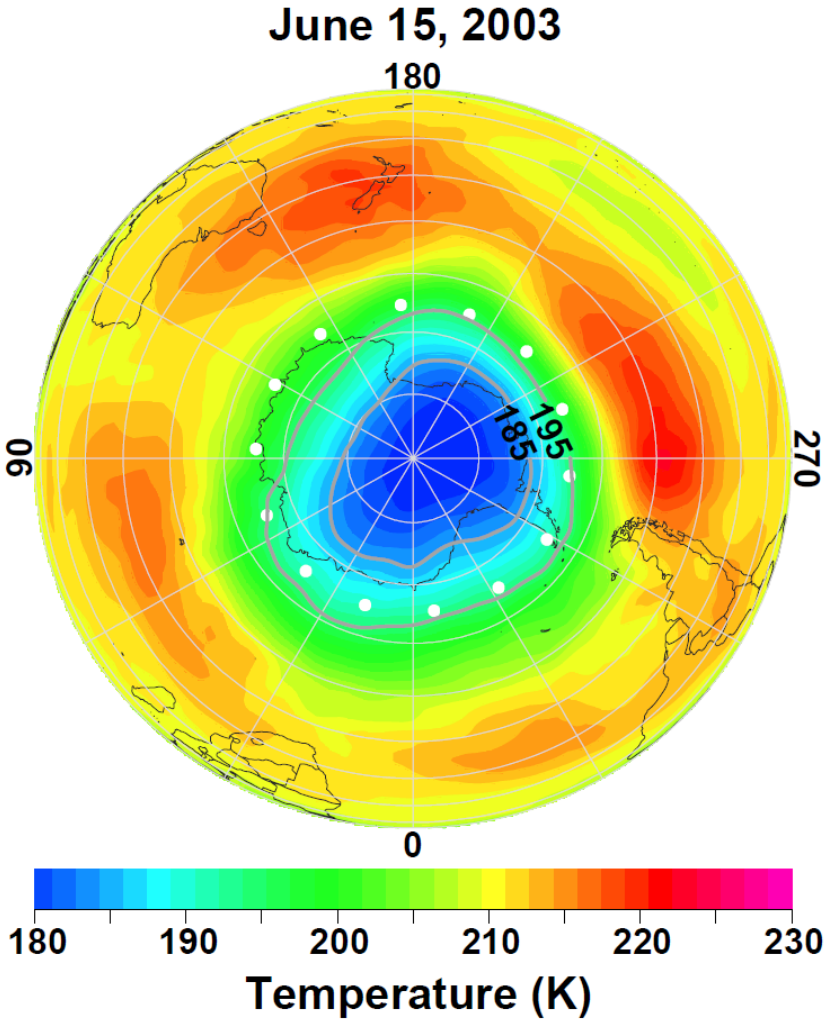

Figure 1: A typical measurement location of ILAS-II a day. A ECMWF temperature map on 490 K (near 20 km) on June 15, 2003 is depicted.

- **Match technique:** To examine time variations in HNO_3 and AEC data measured by ILAS-II, a Lagrangian approach is useful. Analyses were made for five PT levels; initial PT levels with 2 km intervals between 16 and 24 km were taken. For trajectory calculations, the ECMWF operational analysis data were used (6 hourly time resolution and a horizontal resolution of 2.5×2.5 degrees in latitude and longitude). The trajectory calculation for an air parcel was made for **5 days** with a time step of 30 minutes, using diabatic heating rates calculated by *Rosenfield et al.* [1994]. The criteria for time and space for Match pairs are **1 hour and 100 km**, respectively. Only pairs, of which both the forward and backward trajectories met the criteria, were used to tighten the validity of the trajectory. We only show results at 490 K (around 20 km, 36 hPa for temperature of 190 K) where the time variations in HNO_3 and AEC values were most obvious.

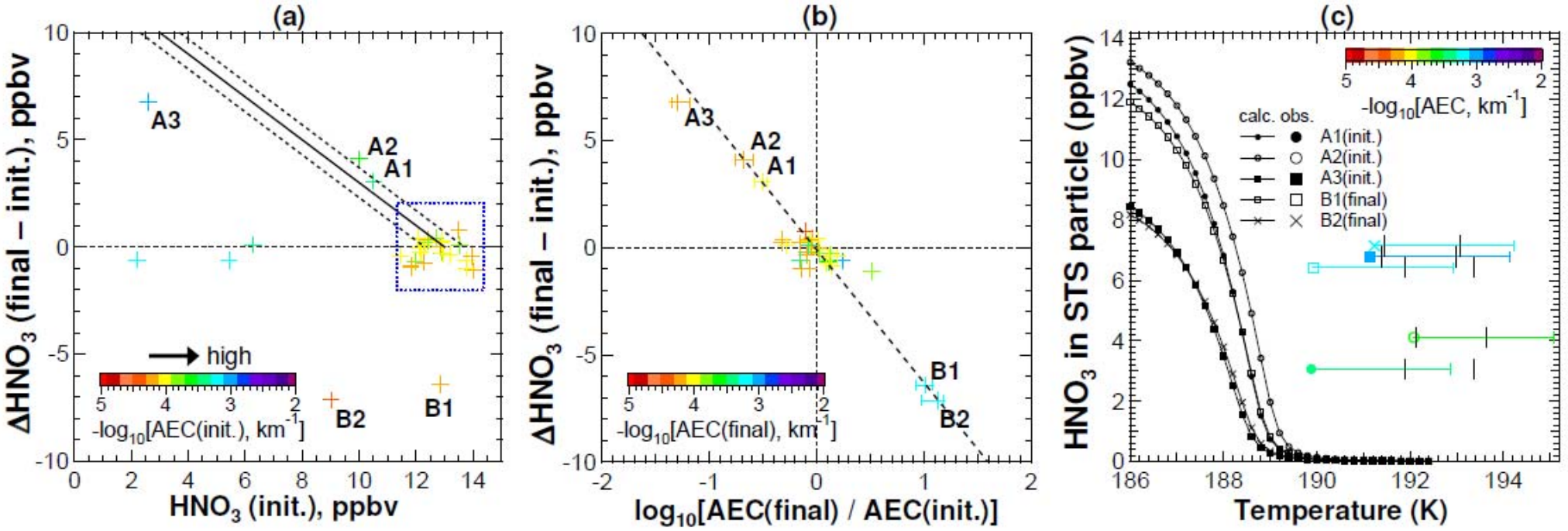

Figure 2: Difference in HNO_3 values at the initial and final times as a function of HNO_3 values at the initial time, **(a)**, and as a function of a ratio of AEC values at the final and initial times, **(b)**. Data points are color-coded by $-\log_{10}$[AEC] value (e.g., 10^{-4} km^{-1} = 4) at the initial time, (a), and at the final time, (b). Results for June 2003 at 20 km are shown. Bars in (b) correspond to error ranges that consider the measurement uncertainties of AEC. **(c)** Calculated HNO_3 values in STS particles as a function of temperature (every 0.2 K) for five temporary denitrification cases. Observed ΔHNO_3 values for those cases are also plotted. Horizontal bars correspond to possible biases in the ECMWF temperatures (cold bias of up to 3 K). T_{NAT} and T_{NAD} values (see Table 1) are shown as vertical bars.

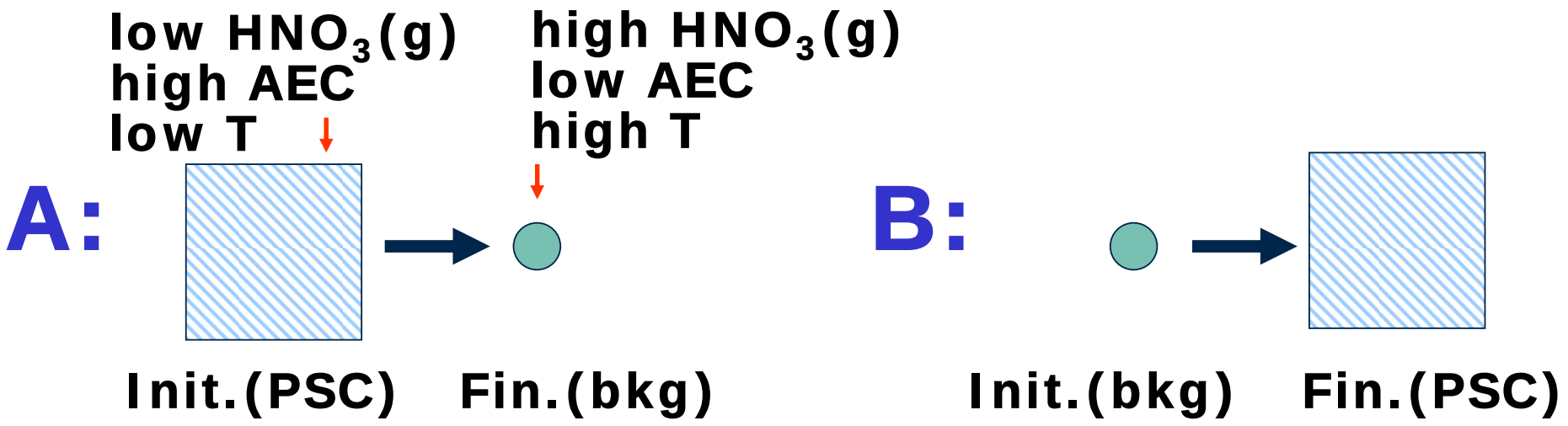

Table 1: Results from several Match pairs that are labeled in Fig. 2. The starting date of trajectories and the matching time (MT), HNO_3, AEC, and temperature between the initial and final measurements are listed. T_{NAT} (and T_{NAD} only for temporary denitrification) is calculated using background HNO_3 values for each cases and an assumed H_2O value of 4 ppmv. The minimum temperature during the Match is also listed. For temporary denitrification, values are shown as blue for clarity.

Case	Date	MT (hours)	HNO_{3ini} (ppbv)	HNO_{3fin} (ppbv)	AEC_{ini} (km^{-1})	AEC_{fin} (km^{-1})	$T_{ini}(T_{NAT}/T_{NAD})$ (K)	$T_{fin}(T_{NAT}/T_{NAD})$ (K)	T_{min} (K)
A1	June 25	57	10.5	13.6	3.6(-4)[a]	1.1(-4)	190(193.4/191.9)	193(193.7)	190
A2	June 25	39	10.0	14.1	3.1(-4)	6.4(-5)	192(193.6/192.1)	201(194.5)	192
A3	June 23	59	2.6	9.4	1.2(-3)	5.9(-5)	191(193.0/191.4)	193(193.3)	190
B1	June 24	79	12.9	6.4	7.2(-5)	7.5(-4)	198(194.1)	190(193.4/191.9)	190
B2	June 22	118	9.0	1.9	4.5(-5)	6.0(-4)	199(193.7)	191(193.1/191.5)	187

[a] Read A(B) as $A \times 10^B$.

- **Results and discussion (RD):** As ILAS-II measured only gas-phase HNO_3, total HNO_3 is not known when HNO_3-containing PSCs occur below T_{NAT}. It is well known that the HNO_3 VMR varies with a thermodynamic equilibrium between gas and liquid (STS) phases (e.g., *Carslaw et al.*, 1995). At 35 hPa for HNO_3 = 13 ppbv, more than 5 ppbv temporary uptake of HNO_3 in STS occurs when ambient temperature cooled to about 188 K (T_{STS}). The NAT particle can also exist below T_{NAT}, though its formation mechanism is still not clear.

  Figures 2a and 2b shows HNO_3 and AEC variations between initial and final locations of each Match pair. Aerosol conditions can be classified into four groups;

  (1) BKG(init.) → BKG(fin.) Blue dotted square

  (2) PSC(init.) → BKG(fin.) Cases A1, A2, and A3

  (3) BKG(init.) → PSC(fin.) Cases B1 and B2

  (4) PSC(init.) → PSC(fin.) ΔHNO3 ≈ 0, high AEC

  We focus on groups (2) and (3) in which large variations of HNO_3 and AEC occurred as "temporary denitrification".

- **(RD cont'd): For five temporary denitrification cases, HNO_3 values in STS particles were calculated (Fig. 2c) [*Carslaw et al.*, 1995]. Whereas, ΔHNO_3 values were also plotted as a measure of degree of temporary denitrification.**

  Disagreement between theory and measurement suggests that PSC particles other than STS caused temporary denitrification, possibly NAT.

  Given particle size distribution for NAT, HNO_3 value in particle can be computed as:

  $$HNO_3\ (\text{ppbv}) = V \cdot d \cdot f \cdot M_{air} / (M \cdot \rho_{air})$$

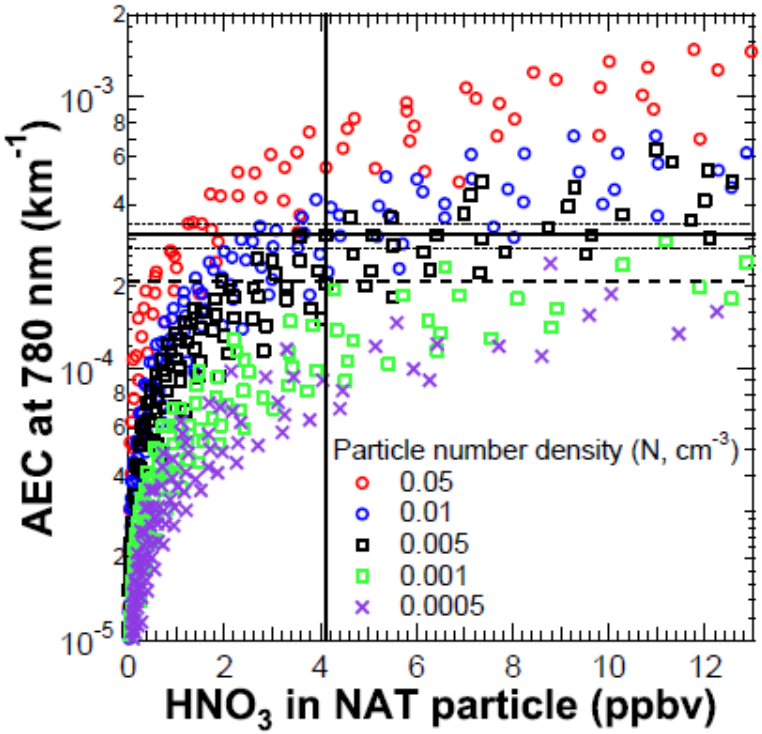

Figure 3: . Calculated AEC values for NAT particles as a function of calculated HNO_3 values in NAT particles at the initial time for the case A2. Different particle number densities are assumed for this calculation with several median radii and widths for the log-normal particle size distribution. A vertical line corresponds to a ΔHNO_3 value for this case. Horizontal lines also correspond to AEC values for this case.

- **(RD cont'd):** where, V is particle volume density, d is density of NAT, f is weight fraction of HNO_3 in NAT, M_{air} is molecular weight of dry air, M is molecular weight of HNO_3, and ρ_{air} is air density.

  Since we have two known parameters (ΔHNO_3 and AEC) for estimating three parameters of PSD (N, r, and σ) for NAT, we assumed probable ranges of them. AEC (at 780 nm) can be calculated on the basis of the Mie theory. An example of the result for the case A2 is shown in Fig. 3.

  In this case A2(init.), the estimated r (σ) ranged from 2.5 ± 0.4 to 1.4 ± 0.3 μm (1.5 to 1.9) for N between 5×10^{-3} and 1×10^{-2} cm^{-3}. We obtained upper limit radii around 2.5 μm for A2(init.). Upper limit particle radii were also obtained for other three Match cases; 2.0, 1.1, and 2.8 μm for A1(init.), B1(final), and B2(final), respectively. Although this is a limited case study, it was found that temporary denitrification by NAT particles with $r \leq 3$ μm could occur when temperatures at the measurements were between T_{NAT} (around 193 K) and T_{STS} (around 188 K) in the beginning of the Antarctic winter vortex.

- **(RD cont'd):** ***Höpfner et al.*** **[2006] also reported that NAT particles with radii smaller than 3 μm were measured with the satellite sensor MIPAS in the same period.**

  Then, we have compared the observed HNO_3 values with the theoretical results using a microphysical box model, which includes nucleation, growth, and sedimentation (Fig. 4). The model utilizes a mechanism that nucleation of NAD on STS droplet surfaces [*Tabazadeh et al.*, 2002] takes place and then instantaneous conversion of NAD nuclei into NAT occurs. A parameterization for the free energy of NAD nucleus formation (ΔG) was performed by sensitivity tests for the five Match cases presented above. For the case A3, good agreement between observed and calculated HNO_3 values was seen for combinations of the ΔG value and the ECMWF temperature of 0.0% / +1K and 2.5% / -1K. Similarly, good agreement was obtained for B2 (0.0% / +1K). For other Match cases, there are some disagreements (up to 35% in HNO_3 values).

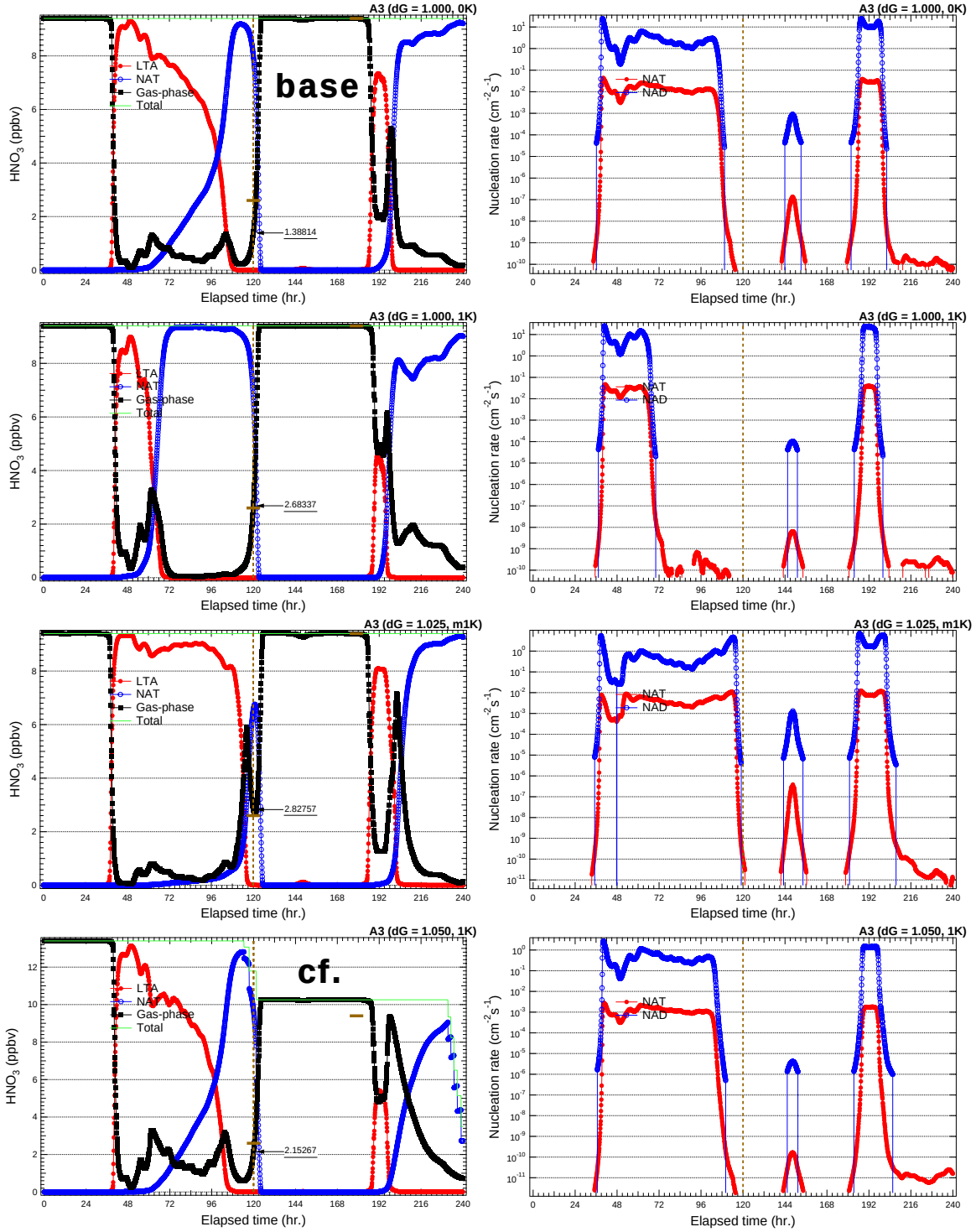

Figure 4: Calculated HNO_3 values for gas and particulate phases using a microphysical box model [*Irie et al.*, 2004] (left-hand column). Sensitivity tests are preformed with ΔG values ranging from 1.000 to 1.100 and temperatures from -2 to +3 K, respectively. The case A3 is only presented, revealing better agreements between measurement and model results than other Match cases. Short horizontal bars reveal the observed HNO_3 values at the initial and the final times. Corresponding variations in the surface nucleation rates for NAT and NAD in STS particles are also presented (right-hand column). The last row is a reference, using a different initial HNO_3 value.

Concluding remarks:

- ILAS-II onboard the ADEOS-II satellite observed the 2003 Antarctic stratosphere from onset through dissipation of the polar vortex [*Nakajima*, 2006; and references therein]. Using these data, short-time (< 5 days) variations of HNO_3 and AEC values were examined by using the Match technique.

- Several Match pairs have revealed decreased HNO_3 values with increased AEC values within the short times, indicating temporary denitrification.

- The observed PSCs could be NAT particles, considering that the temperatures were above existence temperatures for STS, but below those for NAT. Given some size distributions for NAT particles, the median radius of particles was less than 3 micron, although this is a very limited case study.

- The observed HNO_3 values were compared with those calculated by a microphysical box model (MBM), which includes nucleation, growth, and sedimentation.

- For next steps, we will compare the observed AEC values with those calculated by the MBM. ILAS data in June 1997 will be also examined.

References:

Carslaw, K. S., B. P. Luo, and T. Peter (1995), An analytic expression for the composition of aqueous HNO_3-H_2SO_4 stratospheric aerosols including gas phase removal of HNO_3, *Geophys. Res. Lett.*, 22, 1877–1880.

Daerden, F., et al. (2007), A 3D CTM with detailed online PSC-microphysics: analysis of the Antarctic winter 2003 by comparison with satellite observations, *Atmos. Chem. Phys.*, 7, 1755–1772.

Nakajima, H. (2006), Preface to special section on ILAS-II: The Improved Limb Atmospheric Spectrometer–II, *J. Geophys. Res.,* 111, D20S90, doi:10.1029/2006JD007412.

Irie, H., K. L. Pagan, A. Tabazadeh, and T. Sugita (2004), Investigation of polar stratospheric cloud solid particle formation mechanisms using ILAS and AVHRR observations in the Arctic, *Geophys. Res. Lett.*, 31, L15107, doi:10.1029/2004GL020246.

Höpfner, M., et al. (2006), MIPAS detects Antarctic stratospheric belt of NAT PSCs caused by mountain waves, *Atmos. Chem. Phys.*, 6, 1221–1230.

Rosenfield, J. E., P. A. Newman, and M. R. Schoeberl (1994), Computations of diabatic descent in the stratospheric polar vortex, *J. Geophys. Res.*, 99, 16,677–16,689.

Sugita, T., N. Saitoh, S. Hayashida, T. Imamura, K. Saeki, and H. Nakajima (2007), Temporary Denitrification in the Antarctic Stratosphere as Observed by ILAS-II in June 2003, *SOLA*, 3, 137–140, doi:10.2151/sola.2007.035.

Tabazadeh, A., Y. S. Djikaev, P. Hamill, and H. Reiss (2002), Laboratory evidence for surface nucleation of solid polar stratospheric cloud particles, *J. Phys. Chem. A*, 106, 10,238–10,246.